

Real-Time Dynamic Measurements of a Wind Turbine Rotor Blade Using Modal Filtering

Michael Garcia¹, Andrew Reich², Yan-Jin Zhu³, Jonathan White²

¹Department of Mechanical and Aerospace Engineering, Arizona State University, Tempe, Arizona 85287

²Department of Mechanical Engineering, Purdue University, West Lafayette, IN 47907-2031

³Department of Mechanical Engineering, University of Maryland - Baltimore County, Catonsville, MD 21220

ABSTRACT

In 2007, 5,244 MW of new wind power was installed in the United States, or roughly 30% of all new electricity generating capacity, up from only 400 MW in 2002. Recent blade geometries utilize complex shapes to decrease noise and improve performance, but increase the difficulty of load characterization. A practical, real-time approach using modal filtering was developed to monitor the dynamics of 1.8m fiber-composite wind turbine rotor blade using four single-axis accelerometers placed in the span-wise direction. A finite-element model of the blade in the free-free and free-fixed boundary conditions was developed to analyze complex loading patterns. High resolution modal testing and simple electro-dynamic shaker experiments were used to validate the model. A modal filtering method was implemented and demonstrated to provide real-time monitoring of the first four modes of the blade under complicated loading scenarios. This method, scaleable to larger utility-scale turbines, may allow next generation blade designs to incorporate embedded sensors for accurate cycle-based maintenance, as well as aiding in active blade-control schemes.

NOMENCLATURE

MAC	=	modal assurance criterion
η	=	column vector of modal coordinates
x	=	column vector of physical coordinates
C	=	transformation from physical to modal coordinates
ϕ_{pr}	=	p th coefficient of r th modal vector
Φ	=	matrix of modal vectors
*	=	denotes complex conjugates
ANOVA	=	analysis-of-variance method

1 INTRODUCTION

1.1 Background & Motivation

Wind energy is an increasingly economical form of domestic renewable energy with nearly zero total emissions and stable production costs. In recent years US wind energy production has grown by 29% annually. According to the American Wind Energy Association, in 2007 5,244 MW of new wind power was installed in the United States, or roughly 30% of all new national electricity generating capacity, at a total investment of over 9 billion

USD [1]. Recent turbine designs exhibit significantly better performance than early models, but further improvements in energy conversion may be possible with additional research and development.

An increase in wind related research has followed the increase in wind energy demand. Current work is focused primarily on enhancing the performance, reliability, and cost of utility-scale wind turbines. Advancements being investigated include active blade control to decrease fatigue loads and increase energy capture, condition-based maintenance to decrease operational costs, and optimal design to decrease component weight and increase reliability. However, each of these developments requires a fundamental understanding of the blade dynamics of the turbine blades due to operational loading conditions. A blade with integrated sensor measurements may potentially estimate such loads in real-time with higher accuracy than aerodynamic models from cup anemometer/wind vane measurements employed on many current turbines.

1.2 Previous Work

Little previous research has been conducted on techniques for real-time monitoring of wind turbine rotor dynamics under true wind loading. Although much work has been done by the helicopter industry on load characterization, the results are difficult to transfer to wind turbine applications because of vastly different operating conditions [2]. Computational simulations done by Ehlers et al. [3] concluded that loads in the moving reference frame of the blades could be estimated using sensors installed in the fixed reference frame of the turbine structure, but these results were not validated experimentally. Several patents [4, 5] list configurations to measure rotor loads by placing sensors either directly on the blades or indirectly on the drive-train components; however, few systems have been commercialized. Other research has suggested methods for rotor blade load measurement including conventional strain gages, fiber optic strain sensors, accelerometers, and others placed at various locations throughout the rotor and turbine structure [6].

A pseudo inverse modal filter, developed by Zhang, was implemented by Shelley et al. [7] on a five meter truss structure, showing promise for real-time monitoring of the structure. Such a method lends itself well to wind turbine blade applications as it offers real-time, accurate monitoring of blade dynamics, which could be used for cycle-based maintenance or active blade control to reduce fatigue loading. As only the first few modes of a wind turbine are typically of interest, sensor cost is minimal, and sensors imbedded at the factory can be used for multiple purposes beyond only dynamics monitoring, making the method more cost effective. Additionally, a shape-based monitoring technique such as modal filtering, as opposed to frequency-based, may not be as sensitive to environmental effects, and may give better results in complex distributed loading configurations.

2 EXPERIMENTAL PROCEDURE

2.1 Modal Testing

Due to the complex blade geometry of the blade, a high resolution, quasi-2D grid was projected onto the high-pressure surface, from which 92 points were selected for hammer impact measurements, shown in Figure 1. The points mark the accelerometer locations, which were placed at locations of high modal observability. Impact tests showed that a rubber covered plastic tip provided the best input power spectrum to successfully excite higher modes without causing double impacts at the tip of the blade. Two boundary conditions were used in testing the wind turbine blades: free-free and cantilever, shown in Figure 2. The free-free condition exhibited distinct resonant frequencies with low damping characteristics that allowed validation of a computational model, while the cantilever condition better simulated the mounting configuration of the blade on the tower.

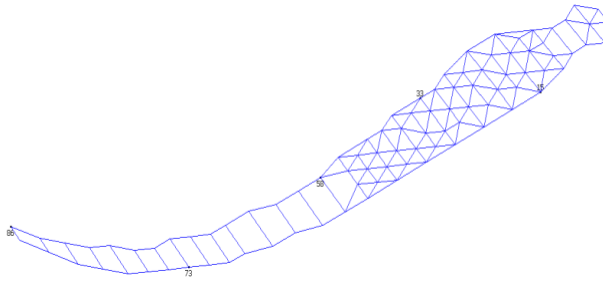


Figure 1: 92 point modal impact grid with accelerometer locations marked.

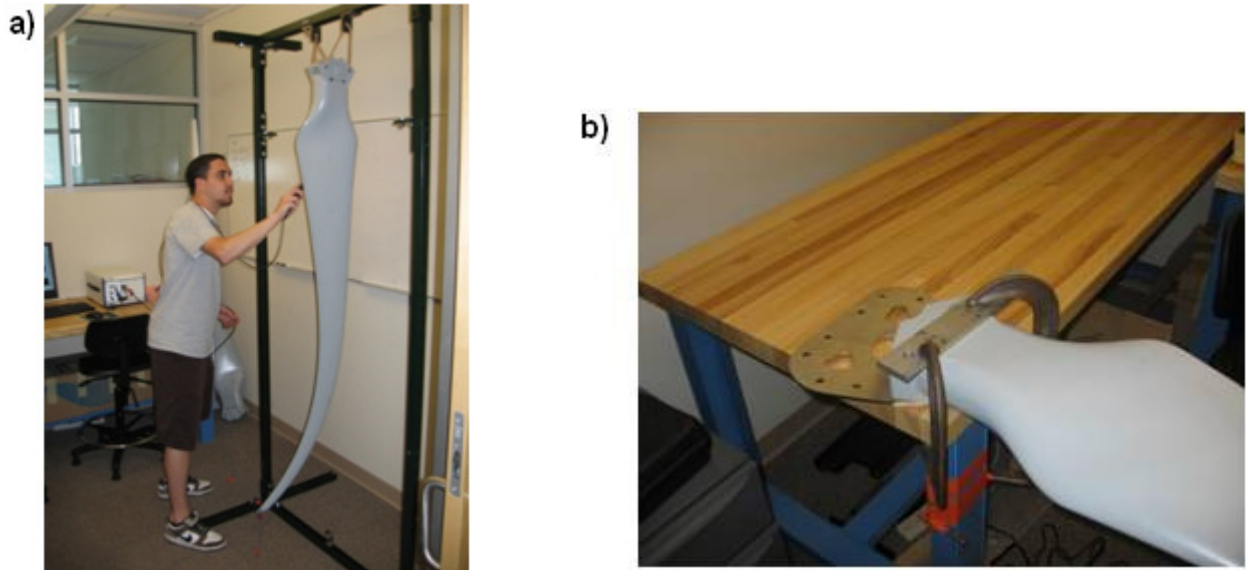


Figure 2: Experimental modal test boundary configurations. a) Free-free testing configuration with the blade suspended from rubber tubing. b) Cantilever configuration with the blade clamped to a semi-rigid table.

2.1.1 Free-Free Boundary Condition

The blade was suspended from rubber tubing to simulate a free-free boundary constraint, shown in Figure 2a. Accelerometers were placed in the flap-wise direction on the high-pressure side of the blade. Flap-wise deflection was deemed most important as other directions contribute little to blade dynamics at low frequencies. Measurements from the high and low-pressure sides were compared, showing that both sides of the blade moved in unison at low frequencies. Initial tests showed that high resolution in the span-wise direction was necessary near the tip to capture bending modes, and high edge-wise resolution was needed near the root to distinguish torsion and drum-like modes. The high-resolution grid made it possible to distinguish a torsional difference between the third and fourth modes, which were very similar in overall shape.

2.1.2 Fixed-Free Boundary Condition

In the cantilever boundary condition, the blade was clamped to the edge of a table as shown in Figure 2b. Although the table was not perfectly rigid and therefore did affect blade dynamics, the major contribution from the table was determined through testing and such modes were subsequently eliminated from future analysis. Due to high damping in the cantilever configuration, only the first four to five modes were easily distinguished in the frequency response data.

2.2 Variability

To identify and quantify the sources of variability, descriptive statistics and analysis-of-variance (ANOVA) were applied to modal tests of several blades. Results indicated blade-to-blade variation dominated unit-to-unit (repeated tests on the same blade) uncertainty, representing at least 90% of variance in frequency across all modes. There was less than 0.15% variation in the resonant frequencies of tests performed on a single blade. Variation due to sensor mounting was shown to be negligible. Due to the variation in blade-to-blade measurements, the dynamics and mode vectors, which are required for the modal filter method, of each blade may be different. Therefore, it may be necessary to perform modal testing on each individual blade to calibrate the modal filter to individual blades.

3 MODEL

3.1 FE Model

A finite-element model of the blade, shown in Figure 3, was created using manufacturer material properties and geometry. To simplify the geometry, only the outer surfaces of the blade were modeled. The top and bottom sections of the geometry were connected with tied nodes to simulate the increased stiffness of the joining surfaces. The model was composed of primarily quadratic shell elements with minimal use of triangular shell elements at complex geometry locations. Mesh density was increased toward the tip of the blade as modal tests showed that dynamics occurred predominantly at this location. In the fixed-free boundary condition, the root surface of the high-pressure side was fixed to simulate the blade clamped to the table.

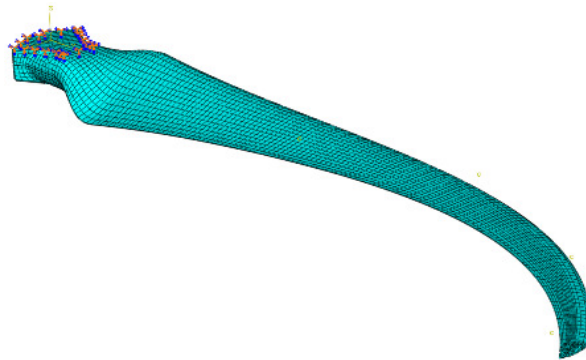


Figure 3: FE model of the blade, showing mesh and fixed-free boundary condition.

3.2 Mesh Verification

A refinement study was conducted to show that the model mesh size was sufficient for convergence. The initial coarse mesh was composed of 9349 elements at an approximate global size of 13 mm (~0.5 inches). A finer mesh was developed using 30406 elements at an approximate global size of 6 mm (~0.25 inches). A comparison of predicted resonant frequencies between coarse and fine meshes of the first five modes for both the free-free and fixed-free boundary conditions is presented in Table 1.

Table 1: Resonant frequency comparison of coarse and fine meshes for cantilever and free-free boundary conditions.

<i>a) Free-Free</i>			
Mode #	Coarse (Hz)	Fine (Hz)	Error
1	29.7	29.8	-0.229%
2	58.9	59.1	-0.386%
3	97.6	97.7	-0.081%
4	109	109	-0.212%
5	141	140	0.447%

<i>b) Fixed-Free</i>			
Mode #	Coarse (Hz)	Fine (Hz)	Error
1	9.15	9.15	-0.014%
2	23.5	23.3	0.541%
3	30.4	30.3	0.250%
4	60.0	60.0	-0.070%
5	95.1	94.9	0.157%

A modal assurance criterion (MAC) between the coarse and fine mesh was also calculated to determine if mode shapes had changed significantly. The MAC for each boundary condition is shown in Figure 4. Mode shape vectors were created using calculated flap-wise deflections at nodes near the accelerometer placements. Along the diagonal, the MAC showed highly correlated values between the two mesh sizes. As the coarse mesh did not show significant deviation from the fine mesh in frequency or shape, the coarse mesh was deemed suitable. The similarity in the mode shapes of the third and fourth modes in the free-free condition (also observed in modal testing), is evidenced by the four high MAC values for these modes. Therefore, it is difficult to distinguish these modes using the selected measurement locations. Other similar modes were observed in the fixed-free condition. This was not considered a major problem, as will be explained in section 4.2.

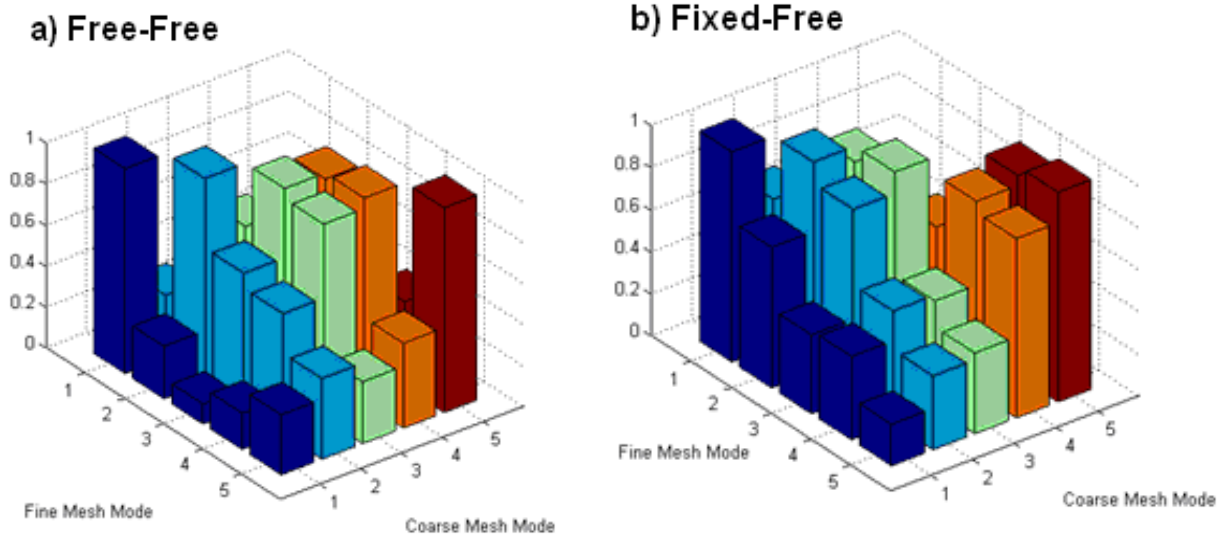


Figure 4: MAC correlation between coarse and fine mesh sizes. a) Free-free boundary condition. b) Fixed-free boundary condition.

3.3 Model Validation

Resonant frequencies predicted by the model are compared to those obtained through experimental testing in Table 2. It should be noted that in the fixed-free condition, the model predicts one more mode than was found experimentally. However, as the additional model mode was very similar in shape to the second model mode, this again was not considered a problem.

Table 2: Resonant frequency comparison of modeled and experimental data for cantilever and free-free boundary conditions.

a) Free-Free			
Mode #	Experimental (Hz)	Model (Hz)	Error
1	25.9	29.7	-14.9%
2	55.3	58.9	-6.42%
3	100	97.6	2.76%
4	115	109	5.53%
5	163	141	13.5%

b) Fixed-Free			
Mode #	Experimental (Hz)	Model (Hz)	Error
1	8.67	9.15	-5.58%
2	24.8	23.5	5.47%
3	n/a	30.4	N/A
4	53.8	60.0	-11.5%
5	86.5	95.1	-9.89%

Although the frequencies deviate slightly at some modes, in the context of modal filtering, the shape of the mode was more important than the resonant frequency. Therefore, as in the mesh refinement study, a MAC comparing the model mode shapes to those determined experimentally, shown in Figure 5, was created. Experimental modal vectors were calculated using accelerometer data, and these were compared to model modal vectors created using flap-wise deflection at nodes near accelerometer placements. From the MAC of the fixed-free configuration, it is clear that the shapes of the first three modes correlate well to experimental results, although the model does not correlate well on the fourth model mode.

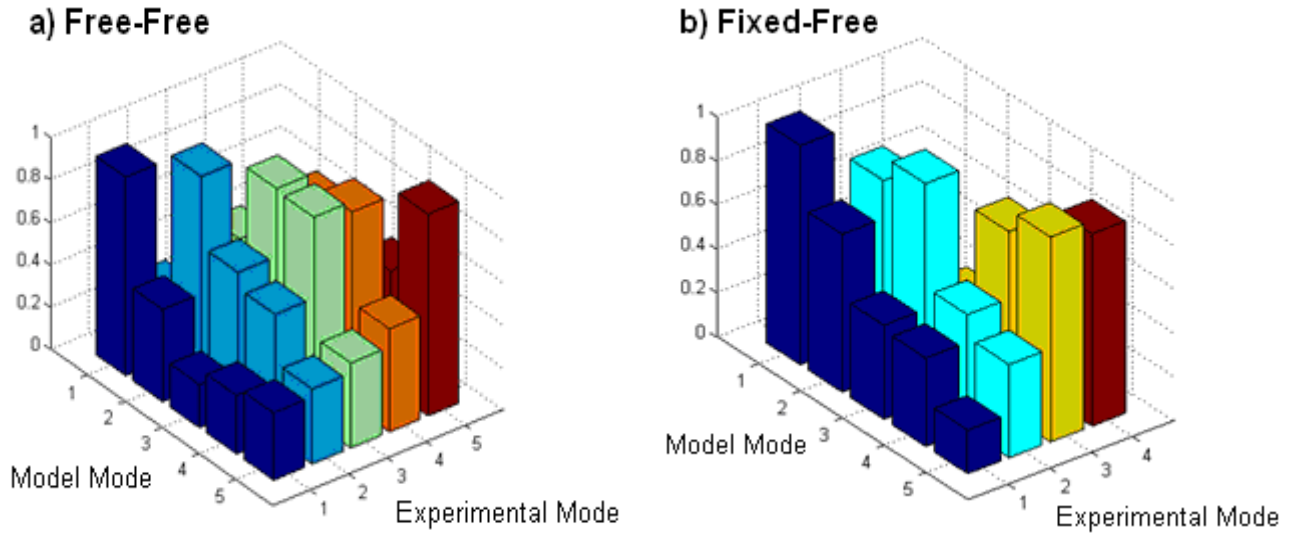


Figure 5: MAC correlations between model and experimental modes. a) Free-free boundary condition. b) Fixed-free boundary condition.

4 MODAL FILTERING

4.1 Pseudo Inverse Modal Filter Method

Modal filtering is a spatial filtering technique which converts a multiple degree of freedom system to a set of single degree of freedom systems. This technique allows real-time dynamics measurement using experimentally derived data [7], as well as giving information about modal participation regardless of forcing frequency.

A modal filter transforms physical coordinates to modal coordinates, as shown in Equation 1.

$$\eta(t) = Cx(t) \quad (1)$$

where x is a column vector of physical outputs from each sensor, η is a column vector of modal coordinates, and C is the transformation matrix, which is also referred to as a modal filter. x can be expressed as a sum of modal vectors where η are the modal coordinates, as in Equation 2.

$$x_j = \sum_{i=1}^N (\eta_i \phi_i + \eta_i^* \phi_i^*) \quad (2)$$

Equation 2 can also be written in matrix form where Φ is a matrix of modal column vectors, determined experimentally from the full scale modal test, and η is the column vector of modal coordinates at a given instant.

$$x = \Phi \eta \quad (3)$$

The modal filter is calculated by forming a pseudo inverse of the modal matrix, Φ . A pseudo inverse Φ^+ may be calculated if the following is true, where I is the identity matrix.

$$I = \Phi^+ \Phi \quad (4)$$

Applying Φ^+ to Equation 3, the pseudo inverse of the modal matrix yields a modal filter which extracts modal coordinates from a vector of responses taken at a given instant in time [7].

$$\Phi^+ x = \eta \quad (5)$$

If the number of sensors matches the number of modes of interest, and all the mode vectors are orthogonal, a standard inverse may be calculated in place of the pseudo inverse. Additionally, if each vector of the modal matrix is scaled to the deflection of a certain sensor location, the modal coordinate is then a measure of the deflection of that mode at that location.

4.2 Experimental Considerations

The number and placement of sensors on the blade is not trivial. As the inverse of the modal matrix was used in the creation of the modal filter, it is important that this matrix be numerically well conditioned. Therefore, in simple terms, sensors must be placed to observe all modes of interest. Kammer [8] proposed an algorithm to optimize sensor placement for large arrays. However, as only four sensors were used on the blade to observe a small number of modes, sensor placement for the blade structure was accomplished by inspection after examining the large-scale modal test results.

Additionally, blade-to-blade variation or environmental changes may lower the effectiveness of the modal filter if the modal matrix changes significantly. Therefore, it is important to test each blade and understand the effects of temperature changes, etc. Shelley et al. [9] proposed an adaptive modal filter technique to compensate for sensor failure or calibration drift, which may mitigate these effects.

For the blade structure, two closely spaced modes were identified. In the flap-wise direction, the shapes of these two modes were nearly identical. Therefore, the modal vectors were linearly dependent, creating a modal matrix that is not full rank and thus noninvertible. To overcome this problem both modes were assumed to be effectively the same and the estimation of their contribution was equivalent to the summation of the contribution of the two independent modes. This method allowed for modal filtering to be performed for three normal modes and one special mode that was a summation of the two similar modes. If the independent contribution of each of the two similar modes was necessary, the locations or number of sensors may need to be modified.

5 RESULTS

5.1 Experimental Results

To determine the effectiveness of the modal filter, a series of sine wave tests were conducted. An electrodynamic shaker was fixed to the tip of the cantilevered blade, as shown in Figure 6, and was subsequently excited with a sine wave at each resonant frequency. A force transducer on the stinger was used to verify force input, and four accelerometers recorded responses along the blade.

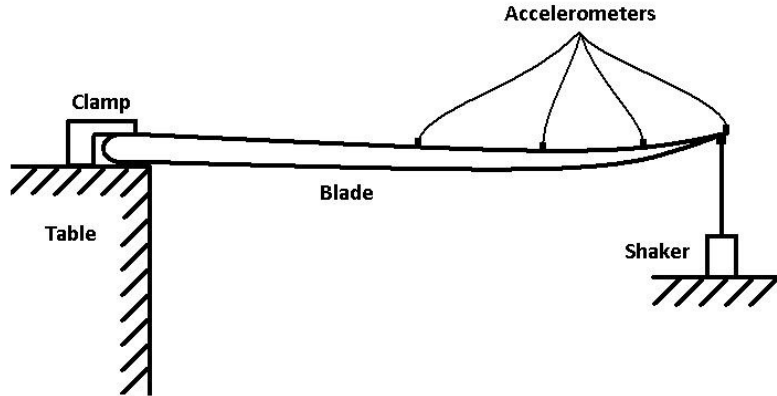
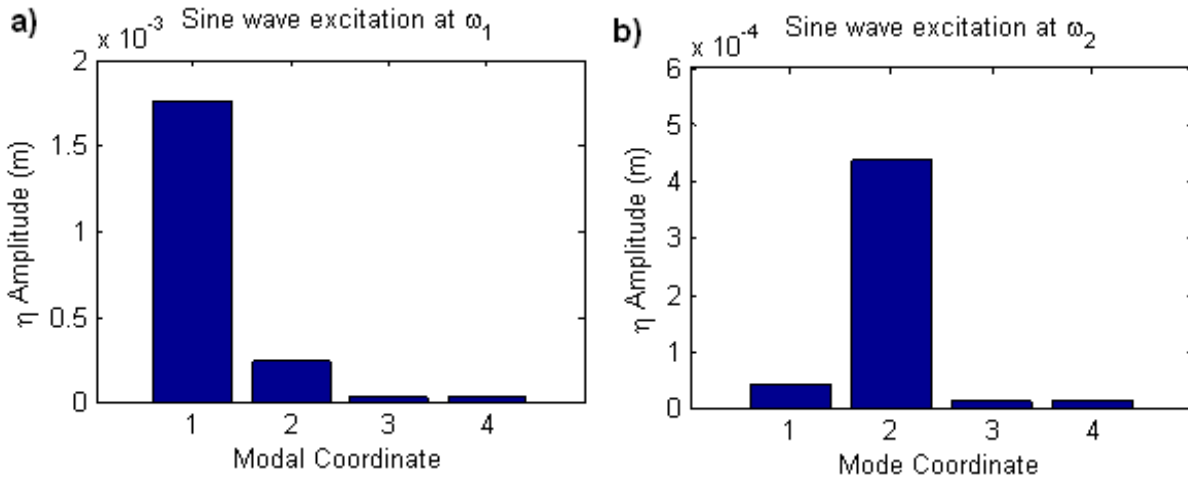


Figure 6: Shaker attachment for sine wave and swept sine excitation.

The accelerometer measurements were integrated twice and filtered to achieve the true deflection, rather than acceleration, of the blade. The pseudo inverse technique was then applied using a modal matrix experimentally determined from modal testing to calculate the modal coordinates. As expected, the modal filter was able to extract the modal coordinate of the mode being excited. The results of the test are shown in Figure 7. The average amplitudes of the modal coordinates over a four-second time interval for each mode are shown for simplification. For example, in Figure 7a, the blade was excited with a sine wave at the first mode resonant frequency, and the modal filter clearly shows that the first modal coordinate (representing the relative participation of the first mode) is dominant. The same is true for the other excitation frequencies, verifying that the modal filter is working as expected.



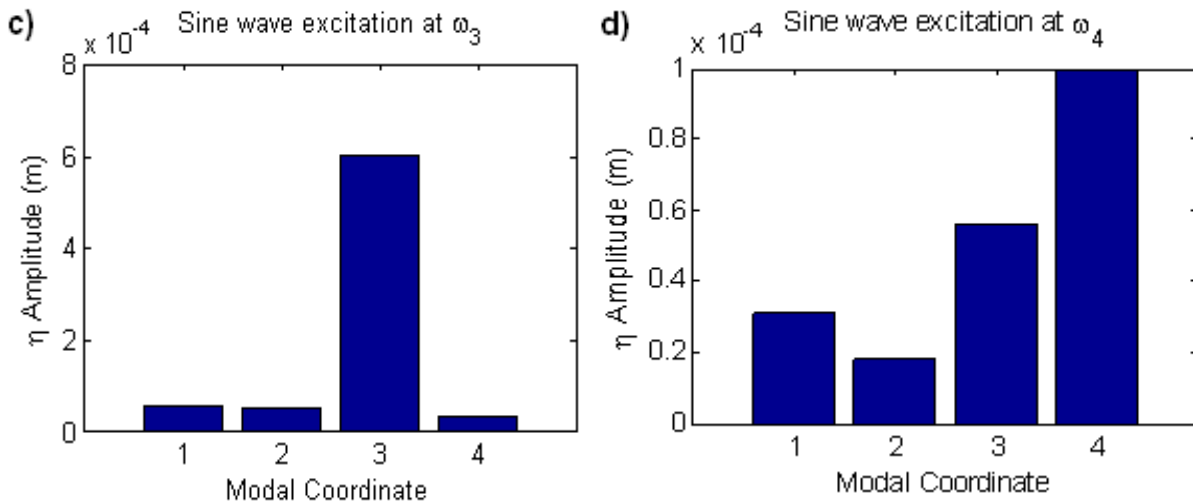


Figure 7: The average amplitude of the modal coordinate shown for modes 1 to 4, a) to d) respectively.

A swept sine input was next applied through the shaker to show the real-time monitoring capabilities of the modal filter method. Figure 8 shows the time history of the calculated modal coordinates, with the resonant frequency of each mode marked in the figure. The amplitude of the mode being excited clearly increased as the input neared that mode's resonant frequency and decreased shortly after. It should be noted that since the modal matrix was scaled to the tip deflection of each mode, the amplitude of the modal coordinate is equal to the tip deflection of that mode. This was done to better facilitate cycle-based condition monitoring of the blade. As higher frequency modes do not deflect as much as lower frequency modes, the corresponding modal coordinates are smaller for high frequency modes.

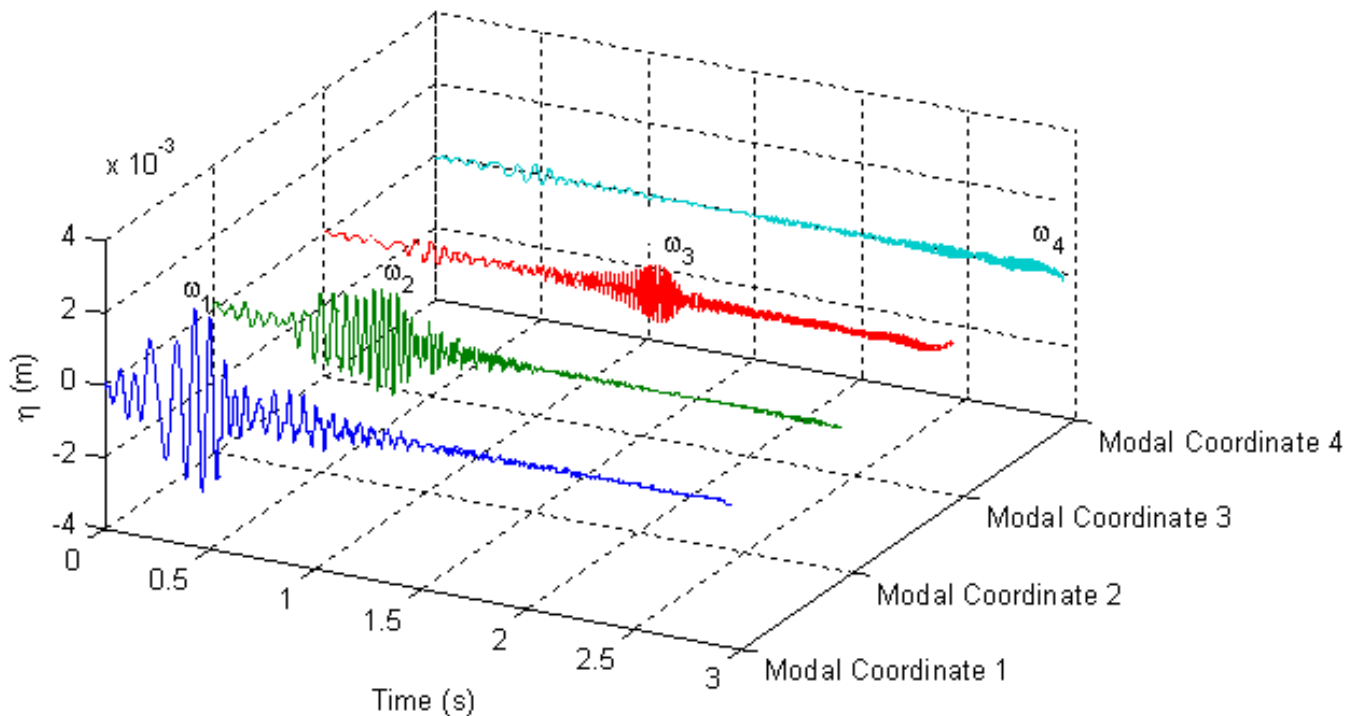


Figure 8: Time history of calculated modal coordinates from swept sine excitation, with approximate resonant frequency of each mode marked.

5.2 Model Prediction

Using the finite element model, the effects of loading configurations that were difficult to reproduce experimentally could be studied in detail. As a first check, the resonant sine wave test was simulated on the model and produced similar results to experimental findings. Next, a node-line excitation was applied. For example, a sine wave force oscillating at the second resonant frequency applied to a node line of the second mode would not excite that mode shape, as shown in the diagram in Figure 9a. Unlike frequency methods, the modal filter method relies only on shape data, and is therefore able to determine that the first mode shape is dominant, even when the forcing is at the second resonant frequency. The modal coordinates, Figure 9b, calculated by the modal filter using acceleration data from the finite element simulation showed that although the force was oscillating at the second resonant frequency, the blade responded primarily in a similar shape to the first mode. For complex wind loadings that exhibit distributed load profiles, this feature of modal filtering may be beneficial for implementing cycle-based maintenance.

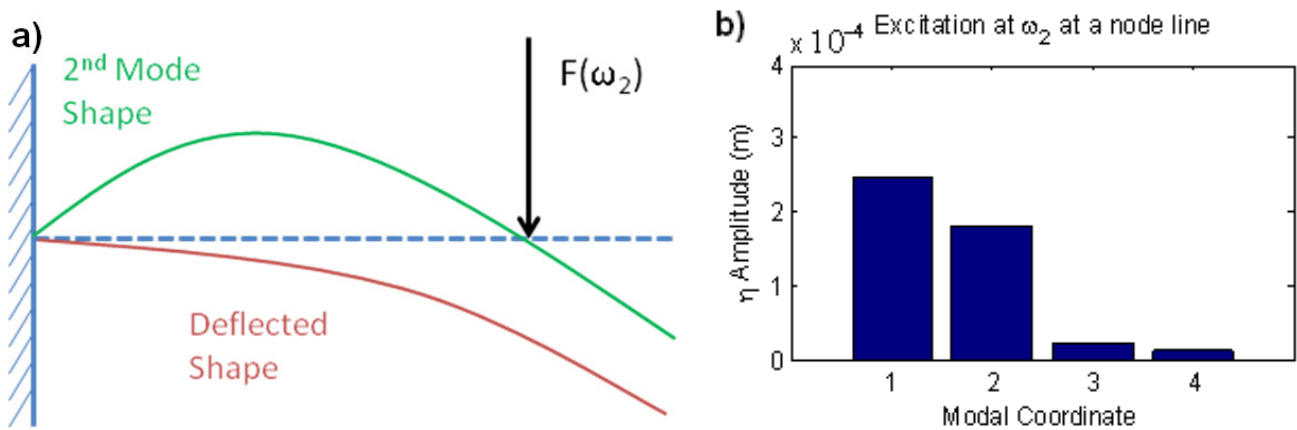


Figure 9: a) Diagram of a node-line loading configuration. b) Calculated average modal coordinate amplitudes showing that the first mode was primarily excited.

As another example of a complex loading configuration, a fourth test was conducted in which two forces at different resonant frequencies but identical amplitudes, shown in Figure 10, were applied to the blade at different points.

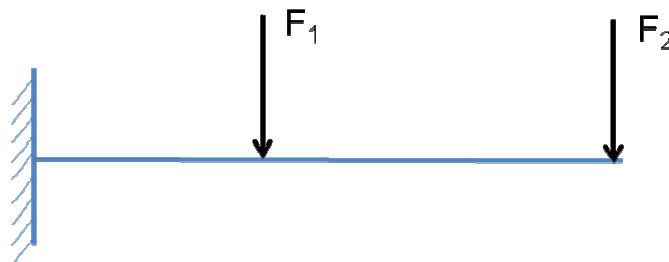


Figure 10: Diagram of approximate location of forces applied to the blade model.

In the first trial, the first resonant frequency was excited at the tip, while the second resonant frequency was excited near the middle of the blade. The modal filter showed that the first mode was primarily excited, while the second mode was hardly excited at all. However, when the first resonant frequency was excited at the middle of the blade and the second resonant frequency was applied to the tip, the first mode was still excited, although at lower deflection, and the second mode was clearly excited, shown in Figure 11. Further investigation would need

to be conducted to understand the consequences of these results. Even more complex forcing profiles, such as distributed wind loadings, could also be investigated using the finite element model.

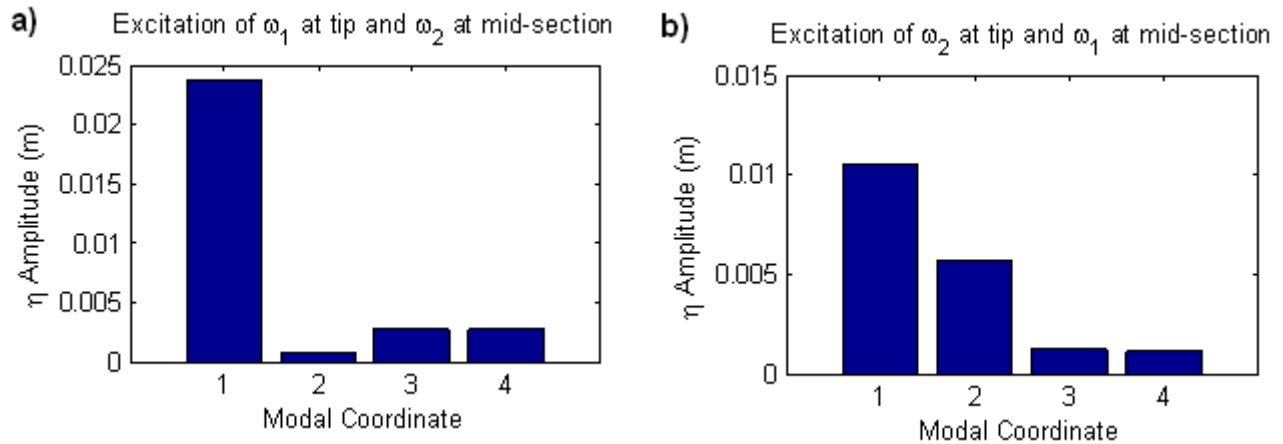


Figure 11: Calculated average modal coordinate amplitudes. a) Excitation of first resonant frequency at the tip and second resonant frequency at the mid-section. b) Excitation of second resonant frequency at the tip and first resonant frequency at the mid-section.

6 CONCLUSIONS

A technique was presented to accurately measure the relative contribution of primary modes of a wind turbine blade under complex loading. This was accomplished using a modal filter method applied to measurements from four single-axis accelerometers placed at high modal observation locations along the span-wise direction of the blade. The modal filtering method has many benefits in structural dynamics measurement. Since the technique does not rely on frequency data or estimation of input forces, it can be implemented in real-time, and is also able to identify modes occurring away from their respective resonant frequencies due to complex loading.

A computational finite element model was developed to aid in the understanding of the blade dynamics and was validated through experimental testing. The computational model was used to predict behavior in experimentally difficult to simulate loading conditions. Wind loading is highly distributed and highly variable, therefore making laboratory tests difficult and expensive. Additionally, utility-scale wind turbine blades can be tens or hundreds of meters long, adding to the difficulty of experimental testing. In future work, the modal filtering technique and model may be applied to understand the dynamics of large structures in operational conditions.

One broader application of the modal filter is cycle-based maintenance. Current maintenance schedules are based on time or revolutions, but due to the variation in wind conditions from one site to another, from turbine to turbine in a particular site, and even from blade to blade on a single turbine, time-based maintenance is costly and inaccurate. By measuring the number of cycles and response amplitude at each cycle a particular mode has been excited, a better estimation of blade fatigue can be achieved. The real-time capabilities of modal filtering also mesh well with other applications such as active blade control to decrease fatigue and increase efficiency.

ACKNOWLEDGEMENTS

Funding for this research was provided by the Department of Energy through the Los Alamos National Laboratory, University of California Interaction Office, and the Department of Energy Enhanced Surveillance Program. The following companies generously provided various software packages to aid in modeling and data analysis: Vibrant Technologies, SIMULIA, and The Mathworks. The authors would like to express their appreciation to Southwest Windpower for providing rotor blades with drawings and specifications for testing, and Dr. Phil Cornwell for his guidance and support. Finally, the authors would like to thank Dr. Charles Farrar and the Los Alamos Dynamics Summer School for the opportunity to conduct this research.

REFERENCES

1. American Wind Energy Association. "Wind Power Outlook 2008: New U.S Capacity by Energy Source." US Energy Information Administration. AWEA. 2008. http://www.awea.org/pubs/documents/Outlook_2008.pdf (accessed June, 2008)
2. Barlas, T K and Van Kuik, G A M. "State of the Art and Prospective of Smart Rotor Control for Wind Turbines." Journal of Physics: Conference Series 75: The Science of Making Torque from Wind. 2007.
3. Ehlers, J., Diop, A., and Bindner, H., "Sensor Selection and State Estimation for Wind Turbine Controls." AIAA Aerospace Sciences Meeting and Exhibit, Reno, NV, 2007.
4. Pierce, Kirk, and Lemieux, David L., "Method and Apparatus for Wind Turbine Rotor Control." U.S Patent: US7160083. Jan. 9th, 2007.
5. Grabau, Peter. "Wind Turbine with Stress Indicator." European Patent EP1075600. August 7th, 2002.
6. Kuhnt, S. Wernicke, J. Shadden, J, and Byars, R., "Advanced Wind Turbine Controls Input Based on Real Time Loads Measured with Fiber Optical Sensors Embedded in Rotor Blades." Paper Presented at the European Energy Conference. Athens, GR. February-March 2007.
7. Shelley, S., Freudinger, L, Allemang, R. J., and Zhang, Q. "Implementation of a Modal Filter on a Five Meter Truss Structure." IMAC IX Conference, Florence Italy. Proceeding Volume 2. p. 1036 - 1044. April 1991.
8. Kammer, D.C., "Sensor Placement for On-Orbit Modal Identification and Correlation of Large Space Structures." Proceedings of the 1990 American Control Conference, San Diego, Ca, May 23-25, pp. 2984-2990.
9. Shelley, S.J., Allemang, R.J., Slater, G.L., and Schultze, F.J. "Active Vibration Control Utilizing an Adaptive Modal Filter Based Modal Control Method." IMAC XI Conference, Kissimee, Florida. pp. 751-758, February 1993.